Supplementary Information for

A novel phosphorus-nitrogen-containing hardener toward anti-flammable, smoke-suppressed and low-dielectric epoxy thermosets

Yu-Ting Yang [a], Hao-Jie Shi [a], Yu Li [a], Yuan Hu [a], Aksam Abdelkhalik [b], Bin Yu [a,*], Xin Wang [a,*]

[a] *State Key Laboratory of Fire Science, University of Science and Technology of China, 96 Jinzhai Road, Hefei, Anhui 230026, P. R. China*

[b] *National Institute of Standards, El-sadat Street, El-Haram, El-Giza, PO Box 136, code 12211, Egypt*

* Corresponding author. E-mail address: yubin@ustc.edu.cn (B. Yu); wxcmx@ustc.edu.cn (X. Wang).

1. Characterization

Proton and phosphorus nuclear magnetic resonance (NMR) spectra were obtained on an AVANCE III 400 NMR spectrometer (Bruker, Germany). Before the measurements, the samples were dissolved in deuterated dimethyl sulfoxide.

Fourier transform infrared (FTIR) spectra were recorded on a Nicolet 6700 spectrometer (Nicolet Instrument Co., USA) using the KBr disc method. The scanning time was 32, and the wavenumber ranged from 4000 to 400 cm−1. In addition, attenuated total reflection (ATR) mode was also conducted with a range from 4000 to 400 cm^{-1}.

The thermal decomposition behavior of the samples was evaluated under a nitrogen atmosphere using a Q5000 thermogravimetric analyzer (TGA) (TA Instruments, USA). The sample (approximately 5.0 mg) was heated from 50 to 700 °C at a ramp rate of 20 °C/min.

The non-isothermal curing kinetics were investigated using a Q2000 differential scanning calorimeter (DSC) (TA Instruments, USA) under nitrogen. The mixture of epoxy monomer and curing agent was heated at various ramp rates of 5, 10, 15, and 20 °C/min. The glass transition temperature (T_g) of the epoxy composites was measured

using a Q2000 differential scanning calorimeter under a nitrogen atmosphere at a heating rate of 10 °C/min.

Dynamic mechanical analysis (DMA) was conducted using a Q800 instrument (TA Instruments, USA) from RT to 200 °C at a heating rate of 5 °C/min in air. A three-point bending mode was used, with a measurement frequency of 1 Hz. The dimensions of the cured samples were 55 mm × 10 mm × 3 mm.

The tensile properties were measured by an electromechanical universal testing machine (MTS Criterion 43, USA) according to the ASTM D3039-08 method, and the test for each sample runs at a speed of 2 mm/min. The average value from at least 5 repetitive measurements was reported. The sample size was 100 mm × 10 mm × 4 mm.

The Charpy impact test of the un-notch samples was carried out on a ZBC1400-A pendulum impact instrument (MTS, China) according to GB/T1043.1-2008. The impact energy was 4 J, and the sample size was 100 mm × 10 mm × 4 mm.

Dielectric properties were measured using a ZJD-C type dielectric constant (D_k) and dielectric loss (D_f) tester (Beijing Zhide, China) at different frequencies. The dimensions of the cured samples were 50 mm (diameter) × 3 mm.

Limiting oxygen index (LOI) measurements were carried out on an HC-2 LOI apparatus (Jiangning, China) following ASTM D2863-97, and the dimensions of the samples were 100 mm × 6.5 mm × 3 mm.

The anti-flammability of the samples was studied using a UL-94 vertical burning chamber following ASTM D3801-20a. The specimen dimensions were 125 mm × 13 mm × 3 mm. The burning behavior of different materials in the vertical orientation was evaluated using a 20 mm blue flame applied in the vertical position. During the test, the flame was applied twice for 10s each. The second flame application was initiated immediately after the first flame extinguished, if ignition occurred, or immediately after the first flame application if ignition did not occur.

Cone calorimeter measurements were performed on a TESTECH cone calorimeter (Suzhou, China) at 35 kW/m^2 following ISO5660-1. The specimens (100 × 100 × 3 mm) were wrapped with aluminum foil, with the top and bottom surfaces covered and the excess foil folded upward around the edges to seal the specimen. The wrapped sample was then placed horizontally in a metal sample holder. A refractory fiber blanket was positioned beneath the specimen as backing insulation, and the holder was secured with a retaining frame to fix the sample during testing.

The morphology of the char residues was observed using an SU8200 field emission scanning electron microscope (Hitachi, Japan) at an accelerating voltage of 3 kV.

The microstructure of the char residues was studied using a LabRAM-HR Confocal Raman Microprobe with a 514.5 nm argon-ion laser.

The elemental composition of the char residues was obtained by an ESCALAB 250Xi X-ray photoelectron spectrometer (XPS) (Thermo Fisher Scientific, USA).

Thermogravimetric analysis coupled with Fourier transform infrared spectrometry (TGA-FTIR) was performed on a Q50 TGA (TA Instruments, USA) connected to an iS50 FTIR instrument (Nicolet, USA) under nitrogen, with heating from room temperature to 800 °C at a ramp rate of 20 °C/min.

2. Results and discussion

We have introduced a comparative system using dimethyl phosphite (DMP) as a phosphorus-only flame retardant. Both the DMP-based and TFDP-based systems were designed with the same base polymer matrix (EP) and identical phosphorus content (2 wt.% P). The DMP-based sample was prepared using the same method as the EP-TFDP sample, as detailed in section 2.3 of the manuscript. The UL-94 rating, limiting oxygen index (LOI), tensile strength, and impact strength were systematically compared. The detailed formulations and corresponding results are summarized in Table S1. Fig. S1 shows the real-time burning photographs of the EP, EP-DMP-2, and EP-TFDP-2 samples during the UL-94 vertical combustion test. The results indicate that, compared with the EP-TFDP system, the EP-DMP system exhibits inferior flame-retardant performance. Specifically, the UL-94 rating decreases from V-0 (EP-TFDP-2) to V-1 (EP-DMP-2), and the LOI value decreases from 28.0% to 26.5%. In addition, the mechanical properties are significantly deteriorated, with both tensile strength and impact strength showing noticeable reductions. These findings clearly demonstrate that

when only a phosphorus component is used, the flame-retardant efficiency is reduced and the mechanical performance is compromised. This can be attributed to that DMP acts as an additive-type flame retardant, which does not chemically bond to the epoxy network during curing and may migrate within the matrix, thereby weakening the mechanical properties. In contrast, TFDP functions as a reactive flame retardant and co-curing agent that is chemically incorporated into the epoxy network. As a result, it delivers more effective flame retardancy along with a better balance of overall properties. This comparison confirms that TFDP is not merely a phosphorus source, but provides a P–N synergistic effect and structural contribution that cannot be achieved by conventional phosphorus additives.

Table S1. Performance Comparison of DMP-based and TFDP-based Systems

Sample	EP (g)	DETDA (g)	DMP (g)	TFDP (g)	P content (wt%)	UL-94	LOI (%)	Tensile strength (MPa)	Impact strength (kJ/m^2)
EP	100	19.61	0	0	0	NR	21.0	37.3	9.5
EP-DMP-2	100	19.61	9.14	0	2	V-1	26.5	39.7	8.9
EP - TFDP-2	100	11.91	0	22.03	2	V-0	28.0	52.7	15.9

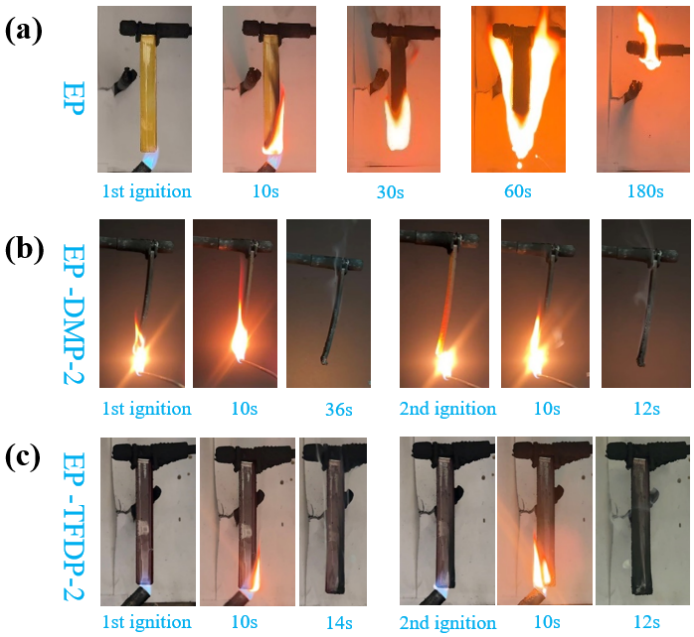

Fig.S1. Real-time photos of UL-94 vertical combustion experiments for (a) EP, (b) EP-DMP-2, and (c) EP -TFDP-2

To ensure a fair and rigorous comparison, we carefully selected representative studies from the literature in which phosphorus-containing amine curing agents were employed in epoxy systems under comparable conditions (similar epoxy matrices such as DGEBA, phosphorus content around ~2 wt.% P, specimen thickness of ~3.0mm, and standardized testing protocols). The relevant data have been summarized in Table S2.

Table S2. Performance Comparison of EP Systems

Sample	EP	P content (wt%)	UL-94	LOI (%)	Δ pHRR (%)	Δ TSP (%)	ΔTHR (%)	Δ Tensile strength (%)	Dielectric constant	Ref.
EP-TFDP-2	DGEBA	2	3mm V-0	28.0	-73.1	-80.8	-48.4	41.3	2.424	This work
EP10/Si-DP7	DGEBA	1.5	3mm V-0	34.7	-43.4	-21.4	-28.7	40.4	Not given	[1]
EP/7.5CPMM/7.5APP	DGEBA	~2.5	3mm V-0	30.5	-81.5	-67.5	-44.0	67.1	Not given	[2]
EP/20%PVDE	DGEBA	1.6	3mm V-0	38.0	-31.3	-6.4	-29.8	24.9	Not given	[3]

EP@ZIF-8@DMMP	DGEBA	1.9	3mm V-1	23.6	-45.5	-28.0	-21.5	-19.0	3.6	[4]
EP/7PPR	DGEBA	~1.5	3mm V-0	32.0	-44.3	-22.2	-13.2	43.1	~2.9	[5]
EP/P1.5	DGEBA	1.5	3mm V-0	33.4	-54.3	12.5	-22.7	Not given	~2.7	[6]
EP/BT15	DGEBA	1.5	3mm V-0	38.0	-28.9	-5.1	-40.7	-4.4	~2.0	[7]
EP@8APP/2PNCo-MOF	DGEBA	2.9	3mm V-0	34.6	-52.8	-48.9	-61.0	-3.7	3.302	[8]
EP/MFR20	DGEBA	1.9	3mm V-0	30.3	-59.5	-37.6	-40.6	4.5	~3.6	[9]

Previous studies have demonstrated that phosphorus-functionalized amine curing systems can indeed achieve excellent flame retardancy. However, these improvements are often accompanied by trade-offs in other key properties. For example: excessive crosslinking may lead to mechanical deterioration or embrittlement of the material. In addition, an increased dielectric constant can limit their applicability in electronic packaging, where low dielectric properties are essential. Furthermore, high loadings of additives or fillers may result in poor dispersion and structural inhomogeneity, thereby adversely affecting the overall performance of the system. These limitations highlight the ongoing challenge of achieving a balanced combination of flame retardancy and multifunctional properties. In contrast, the primary objective of this work is not to maximize a single parameter (e.g., LOI or ΔTHR), but to achieve a balanced multifunctional performance, including flame retardancy, mechanical strength, and dielectric reliability. This balance is particularly critical for advanced applications such as battery encapsulation materials.

Through the above controlled experimental comparisons and literature comparisons under similar conditions, the TFDP-based formulation demonstrates a

well-balanced performance in terms of flame retardancy, thermal stability, mechanical and dielectric properties, highlighting its strong competitiveness. Therefore, the performance improvements reported in this study are not merely speculative, but are supported by both experimental evidence and systematic comparisons.

[1] M. Chai, H. Liu, Y. Wu, K. Xue, P. Zhang, L. Liu and Y. Huang, Chemical Engineering Journal, 2024, 493, 152785.

[23] Y. Li, Z. Yang, J. Guan, Q. Yan and Z. Lei, International Journal of Biological Macromolecules, 2025, 309, 142579.

[3] Y. Q. Liu, H. Liu, S. Lin, J. B. Zang, S. Xu, Y. Yang and L. Shang, Materials Today Chemistry, 2026, 52, 103398.

[4] H. R. Guan, T. S. Liu, L. F. Shi, L. W. Ma, A. M. Kirillov, W. S. Liu, L. Z. Yang and W. Dou, New Journal of Chemistry, 2024, 48, 5745-5759.

[5] W. J. Yang, Q. J. Wu, Y. Zhou, S. E. Zhu, C. X. Wei, H. D. Lu, W. Yang and R. K. K. Yuen, Progress in Organic Coatings, 2024, 186, 107967.

[6] J. Liu, M. Wu, Z. Fu, J. Liu, G. Yu, Q. Yu, Y. Han and Z. Wang, Polymer, 2024, 305, 127173.

[7] Y. W. Mao, H. P. Cai, L. H. Gao, W. Y. Huang and X. Huang, Reactive & Functional Polymers, 2023, 193, 105762.

[8] J. P. Huang, X. W. Yang, Y. Zhu and G. Y. Wang, Acs Applied Engineering Materials, 2024, 2, 2324-2337.

[9] B. Y. Jiang, Y. X. Zhang, J. Gao, Y. T. Guo, J. Ying, G. H. Chen, J. H. Han, Y. M. Zhao, T. Y. Gao, Y. Z. Wang, Q. Wu, Y. M. Yu, S. N. Li and J. F. Dai, International Journal of Biological Macromolecules, 2024, 277.

Table S3. Materials Classifications

Criteria Conditions	V-0	V-1	V-2
Afterflame time for individual t_1	≤ 10 s	≤ 30 s	≤ 30 s
Afterflame time for individual t_2	≤ 10 s	≤ 30 s	≤ 30 s
Total afterflame time per set $\sum(t_1 + t_2)$ for 5 specimens	≤ 50 s	≤ 250 s	≤ 250 s
Afterflame + afterglow $t_2 + t_3$ for each specimen	≤ 30 s	≤ 60 s	≤ 60 s
Cotton indicator ignited by flamingparticles or drops	No	No	Yes
Afterflame or afterglow of any specimenNoup to the holding clamp	No	No	No